Progress In Electromagnetics Research M, Vol. 106, 93–104, 2021

Design and Optimization of a TEM Cell Structure Suitable for Wider Bandwidth

Ting Zhou[1], Xinwei Peng[1], Shoukun Huang[1], Jicong Zhao[1, 2], and Haiyan Sun[1, 2, *]

Abstract—Transverse electromagnetic (TEM) cell is usually used to evaluate the electromagnetic immunity and electromagnetic radiation disturbance of the equipment under test (EUT) and integrated circuit (IC). Affected by the structure of the TEM cell, high-order modes and reflection will be generated in the high frequency range, which will limit the higher frequency applications of the TEM cell. In this paper, the TEM cell specified in IEC61967-2 standard is improved by adopting several methods, including segmented impedance matching, slitting outer conductor, slotting inner conductor, adding absorbing materials, and adding an external shielding box. The results show that the improved TEM cell voltage standing wave ratio (VSWR) is less than 1.2 in 0–3.4 GHz, less than 1.3 in 0–3.75 GHz, and less than 1.5 in 0–4.06 GHz; at the same time, the S-parameter characteristics are better.

1. INTRODUCTION

With the development of electromagnetic compatibility (EMC) detection technology, people are looking for a more convenient method for detecting EMC of electronic devices. TEM cell is an effective device used for EMC testing in recent years. Compared with other devices, TEM cell has the advantages of low cost and easy use. For some small electronic products, TEM cell can be used for electromagnetic immunity test and electromagnetic radiation disturbance test.

The TEM cell is essentially a deformed coaxial line and consists of a main transmission section and two tapered transition sections [1]. The basic principle is to generate transverse electromagnetic wave between the inner and outer conductor plates of the cell. The electromagnetic field distribution in the cell is the same as that in the general coaxial line. The electromagnetic radiation characteristics of the EUT can be measured when EUT is fixed on the top of the middle section of the cell, so that the field strength can be accurately calculated. The TEM cell structure of IEC61967-2 standard is shown in Fig. 1 [2]. All the metallic parts in the model are considered to be copper. The overall dimension is 33.8 cm × 15.2 cm × 9.9 cm, and the test frequency range is 150 kHz–1 GHz. The main disadvantages of TEM cell are that it will produce high-order modes and reflection in a certain frequency band, which seriously affect the cell performance and limit the upper limit of cell usage frequency [3, 4].

In order to suppress the high-order modes and improve the upper limit of frequency, scientists have carried out a lot of research without changing the overall size of the cell. Luo et al. studied the structure of three strip-line TEM cells and the methods of expanding the operating frequency [5]. Arezoomand et al. compared two methods of changing the inner conductor and concluded that the piecewise linear method could better improve the matching bandwidth [6]. Crawford et al. studied the method that adding absorbing materials to the TEM cell can suppress the high-order modes and resonance [7]. Walter and Leat slit the inner conductor of the asymmetric TEM cell and placed resistors in the center of the slits, which effectively weakened the TE_{111} mode resonance [8]. Methods in [5–8] improve the matching

Received 15 August 2021, Accepted 2 December 2021, Scheduled 14 December 2021

* Corresponding author: Haiyan Sun (sun.yan@ntu.edu.cn).

[1] School of Information Science and Technology, Nantong University, Nantong, China. [2] State Key Laboratory of Transducer Technology, Shanghai, China.

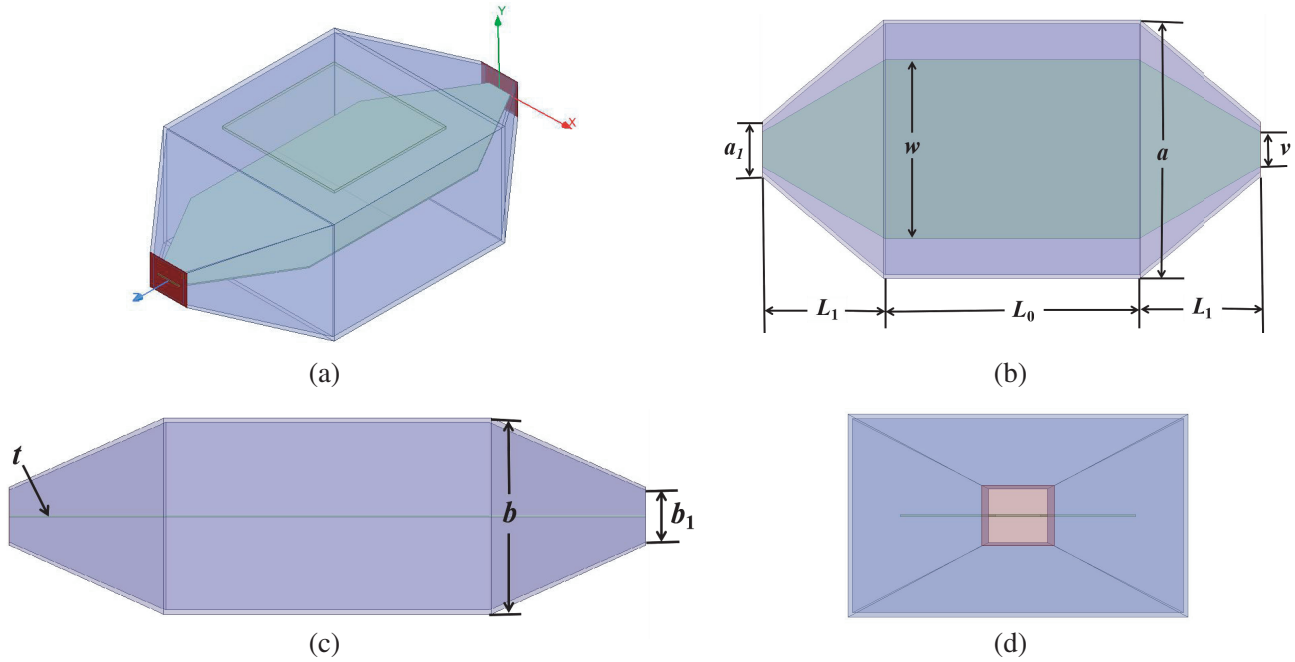

Figure 1. The TEM cell structure of IEC61967-2 standard. (a) Overall model. (b) Top view. (c) Front view. (d) Side view.

performance of the TEM cell and suppress the high-order modes to a certain extent. In this paper, the TEM cell specified in IEC61967-2 standard is improved by adopting several methods, including segmented impedance matching, slitting outer conductor, slotting inner conductor, adding absorbing materials, and adding an external shielding box. The results show that the improved TEM cell VSWR is less than 1.2 in 0–3.4 GHz, less than 1.3 in 0–3.75 GHz, and less than 1.5 in 0–4.6 GHz; at the same time, the S-parameter characteristics are better.

2. TEM CELL DESIGN

2.1. Segmented Impedance Matching Design

Characteristic impedance is one of the main performance parameters of the TEM cell, and good impedance matching must be ensured in the design. In theory, the TEM cell should maintain 50 Ω impedance matching to accommodate the connection with the coaxial connectors. In the case that the size of the outer structure of the TEM cell is determined, the size of the inner conductor can be appropriately adjusted to achieve impedance matching. This paper adopts the methods of segmented impedance matching, formula calculation, and simulation analysis to realize it.

2.1.1. Middle Section Design

Firstly, the middle section of the TEM cell is designed for impedance matching. The middle section model can be approximately equivalent to a rectangular coaxial line. According to IEC61967-2 standard, the length of outer conductor $L_0 = 152$ mm, $L_1 = 93$ mm, width $a = 152$ mm, height $b = 99$ mm; the length of inner conductor $L_0 = 152$ mm, $L_1 = 93$ mm, thickness $t = 1$ mm. To match the impedance to 50 Ω for best performance, the width w of the inner conductor must be obtained.

The calculation formula of characteristic impedance Z_1 in the middle section of the TEM cell is approximately equivalent to:

$$Z_1 = \frac{\sqrt{\varepsilon_0 \mu_0}}{c_0} = \frac{\varepsilon_0 \eta_0}{c_0} \tag{1}$$

where μ_0 is the permeability of vacuum; ε_0 is the dielectric constant of vacuum; η_0 is the free space characteristic impedance; c_0 is the unit distributed capacitance, and the unit is F/m.

The calculation formula of the distributed capacitance per unit length c_0 is approximately equivalent to [9]:

$$\frac{c_0}{\varepsilon_0} = 4\left[\frac{w}{b} + \frac{2}{\pi}\ln\left(1 + \coth\frac{\pi\,(a-w)}{4b}\right)\right]\left(a \geq b, w \geq \frac{1}{2}b\right) \tag{2}$$

From Equation (1) and Equation (2), we can get [10]:

$$Z_1 = \frac{30\pi}{\left[\frac{w}{b} + \frac{2}{w}\ln\left(1 + \coth\frac{\pi\,(a-w)}{4b}\right)\right]} \tag{3}$$

The outer conductor parameters a and b have been determined. Assume that the value of characteristic impedance Z_1 is 50 Ω. Substituting these values into Equation (3), the calculated value of the inner conductor width $w = 103.6$ mm can be obtained. According to the preliminary calculated value, the simulation model of the middle section of the TEM cell is established in high frequency structure simulator (HFSS). The transient impedance Z_1 of the middle section when $w = 103.6$ mm is shown in Fig. 2, and the maximum value of Z_1 is 51.03 Ω. In order to obtain a better impedance matching effect, a better value of w needs to be obtained.

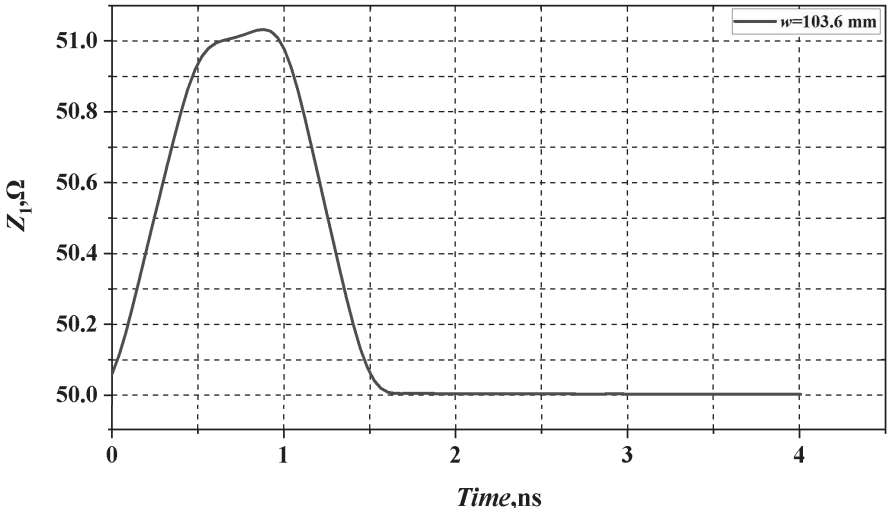

Figure 2. The transient impedance Z_1 of the middle section when $w = 103.6$ mm.

The formula of parallel plate capacitor is approximately equivalent to:

$$c = \frac{\varepsilon s}{d} \tag{4}$$

According to Equation (4), increasing the relative area between two conductors or reducing the distance between two conductors can effectively increase the parasitic capacitance. Therefore, increasing the width of the inner conductor in the middle section can reduce the characteristic impedance. In HFSS, regard w as a variable, and observe the relationship between w and Z_1. The transient impedance Z_1 of the middle section varies with the width w, shown in Fig. 3. When $w = 105.6$ mm, the transient impedance Z_1 is closest to 50 Ω.

2.1.2. Tapered Transition Section Design

Next, the tapered transition section of the TEM cell is designed. When satisfying:

$$\frac{v}{w} = \frac{a_1}{a} \tag{5}$$

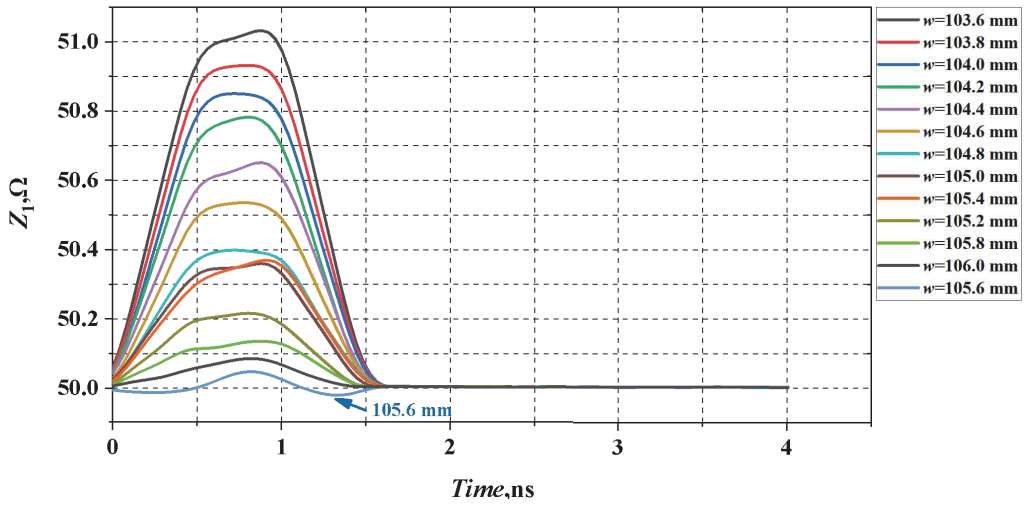

Figure 3. Variation curves of Z_1 with w.

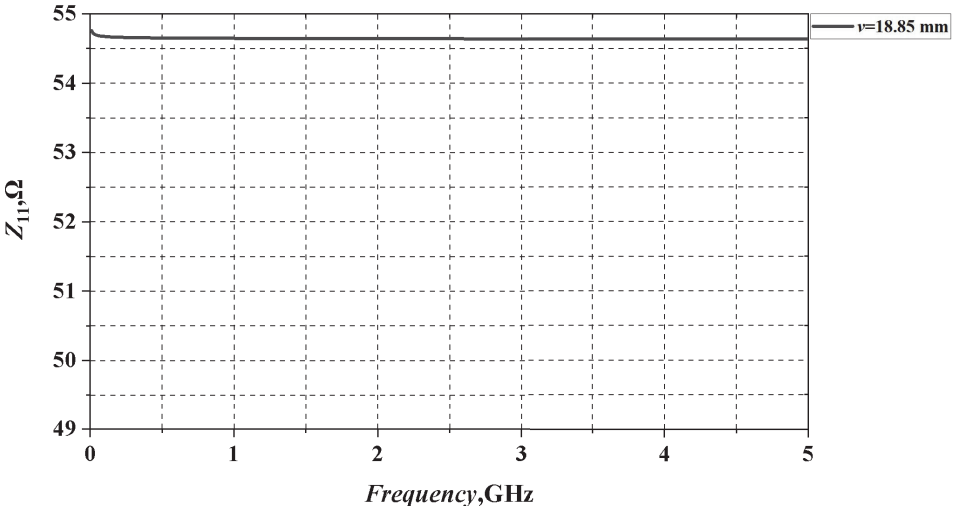

Figure 4. The port impedance Z_{11} of the transition section when $v = 18.85\,\text{mm}$.

the impedance matching effect is better. Here, the width of the outer conductor end of the transition section $a_1 = 32.5\,\text{mm}$, which can be well connected with the actual N-type connector. When $w = 105.6\,\text{mm}$, according to Equation (5), the width of the inner conductor end of the transition section $v = 18.85\,\text{mm}$. The transition section model is a nonuniform coaxial structure. In particular, the port impedance of transition section should meet the requirement of $50\,\Omega$, which is suitable for $50\,\Omega$ coaxial connector termination. The port impedance Z_{11} of the transition section when $v = 18.85\,\text{mm}$ is shown in Fig. 4, and the value of Z_{11} is $54.66\,\Omega$. In HFSS, regard v as a variable, and observe the relationship between v and Z_{11}. The port impedance Z_{11} varies with the width v, shown in Fig. 5. When $v = 20.25\,\text{mm}$, the port impedance Z_{11} of the transition section is closest to $50\,\Omega$.

The traditional linear thinning inner conductor structure cannot meet the matching condition of transition section. From the perspective of time domain, the transient impedance Z_2 of the transition section when $v = 20.25\,\text{mm}$ is shown in Fig. 6, and the minimum value of Z_2 is $47.90\,\Omega$. Therefore, without changing the port impedance, the edge of the inner conductor of transition section can be adjusted by slotting to match the impedance. The inner conductors and the transient impedances of the transition section before and after adjustment are shown in Fig. 7. The minimum value of transient impedance Z_2 increases from the initial $48.60\,\Omega$ to the adjusted $49.17\,\Omega$.

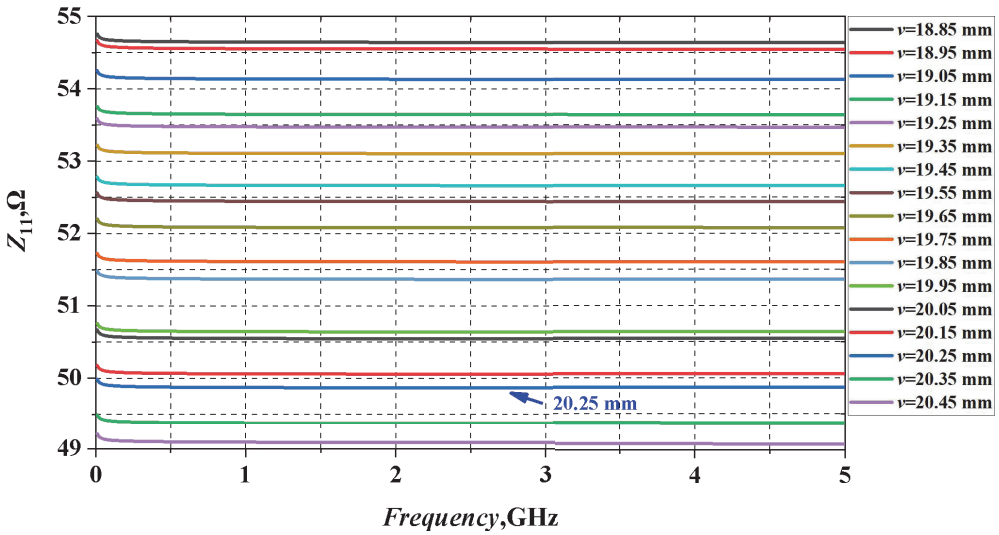

Figure 5. Variation curves of Z_{11} with v.

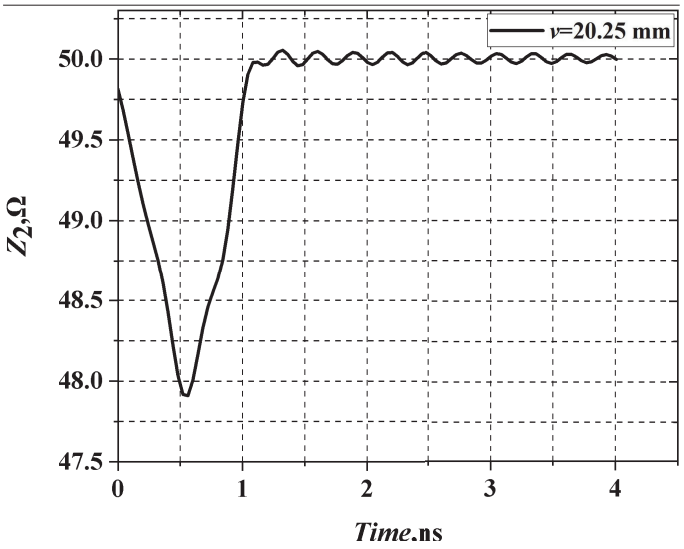

Figure 6. The transient impedance Z_2 of the transition section when $v = 20.25\,\text{mm}$.

2.2. Overall TEM Cell

The above-mentioned rectangular middle section and tapered transition sections are combined to obtain a preliminary designed TEM cell. The preliminary designed TEM cell and performance curves are shown in Fig. 8. According to Fig. 8, the overall impedance matching is good. However, in the range of 0–3 GHz, return loss (S_{11}) has two resonance peaks: P_1 and P_2. The value of peak P_1 is -5.24 dB at 1.85 GHz, and the value of peak P_2 is -0.63 dB at 2.63 GHz. At the same time, the corresponding VSWRs are 3.41 at 1.85 GHz and 25.89 at 2.63 GHz. Compared with IEC61967-2 standard, the TEM cell completed in the preliminary design meets the VSWR of less than 1.5 when the usage frequency is less than 1.85 GHz.

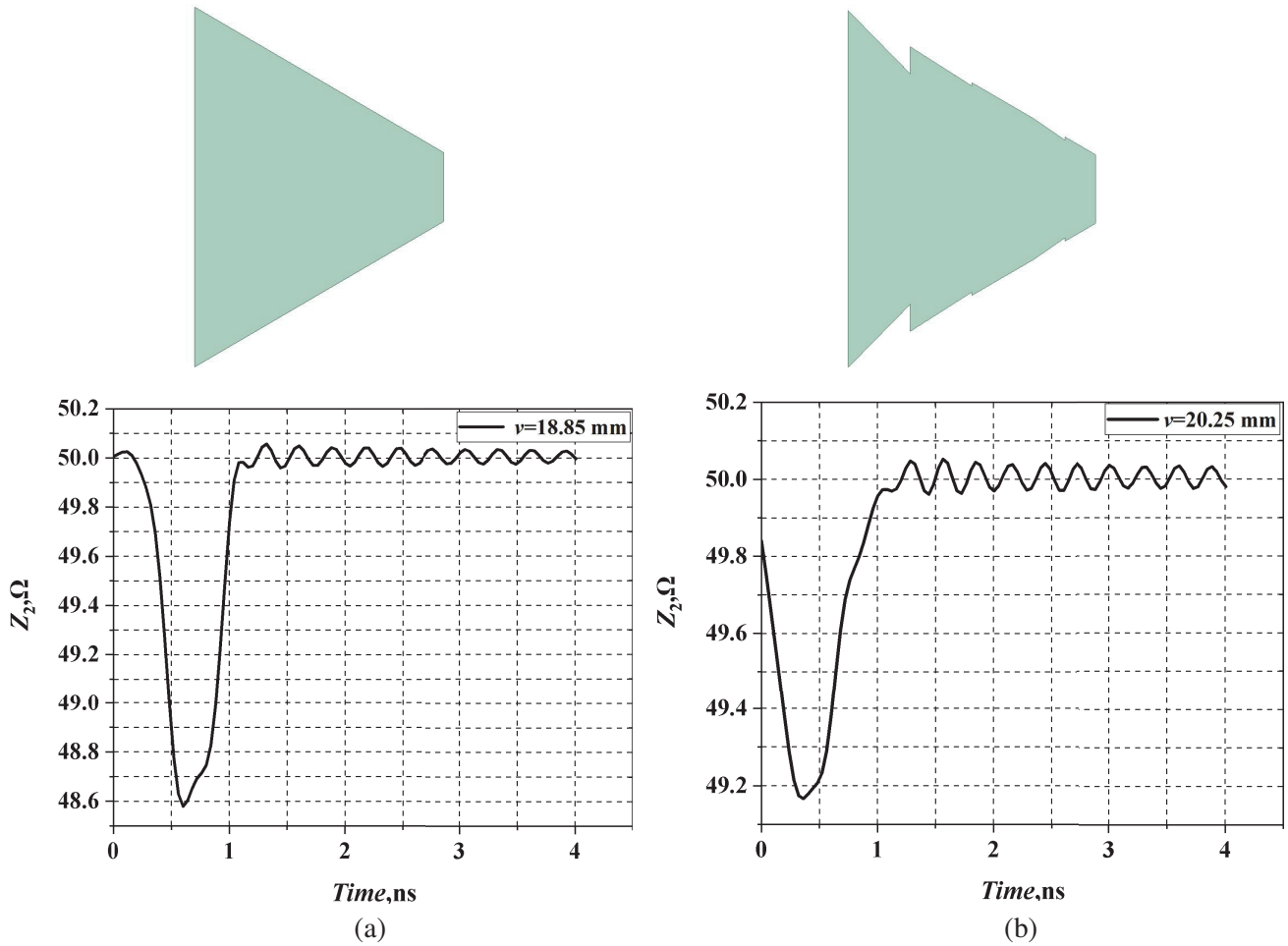

Figure 7. The inner conductors and transient impedances Z_2 of the transition section before and after adjustment. (a) Before conductor adjustment. (b) After conductor adjustment.

3. TEM CELL OPTIMIZATION

After completing the above impedance matching design, in order to improve the upper frequency limit of TEM cell, it is necessary to analyze the high-order modes and reflection to optimize TEM cell.

3.1. High-Order Modes Suppression

The main mode of transmission waves in TEM cell is transverse electromagnetic. Electric field components and magnetic field components are perpendicular to the propagation direction of the electromagnetic wave (z-axis), and the direction of the currents and magnetic field follows the right-handed spiral rule, so the currents on the shell surface flow along the z-axis [11]. Due to the structure, TEM cell will produce high-order modes at a certain frequency. According to Fig. 8, at resonance peak P_1, S_{11} is -5.24 dB, and VSWR is much larger than 1.5 dB, so most of the energy is reflected back, which indicates that P_1 is the frequency point of the first high-order mode in TEM cell. The main high-order mode in TEM cell is transverse electric (TE) mode. Although the magnetic field of TE contains the components perpendicular to the propagation direction, the main components are along the propagation direction of the wave. According to Maxwell's equation, in TE mode, the direction of currents on the shell surface is perpendicular to the direction of magnetic field. Slotting along the z-axis will cut off the current of high-order modes and will not destroy the transmission of TEM in

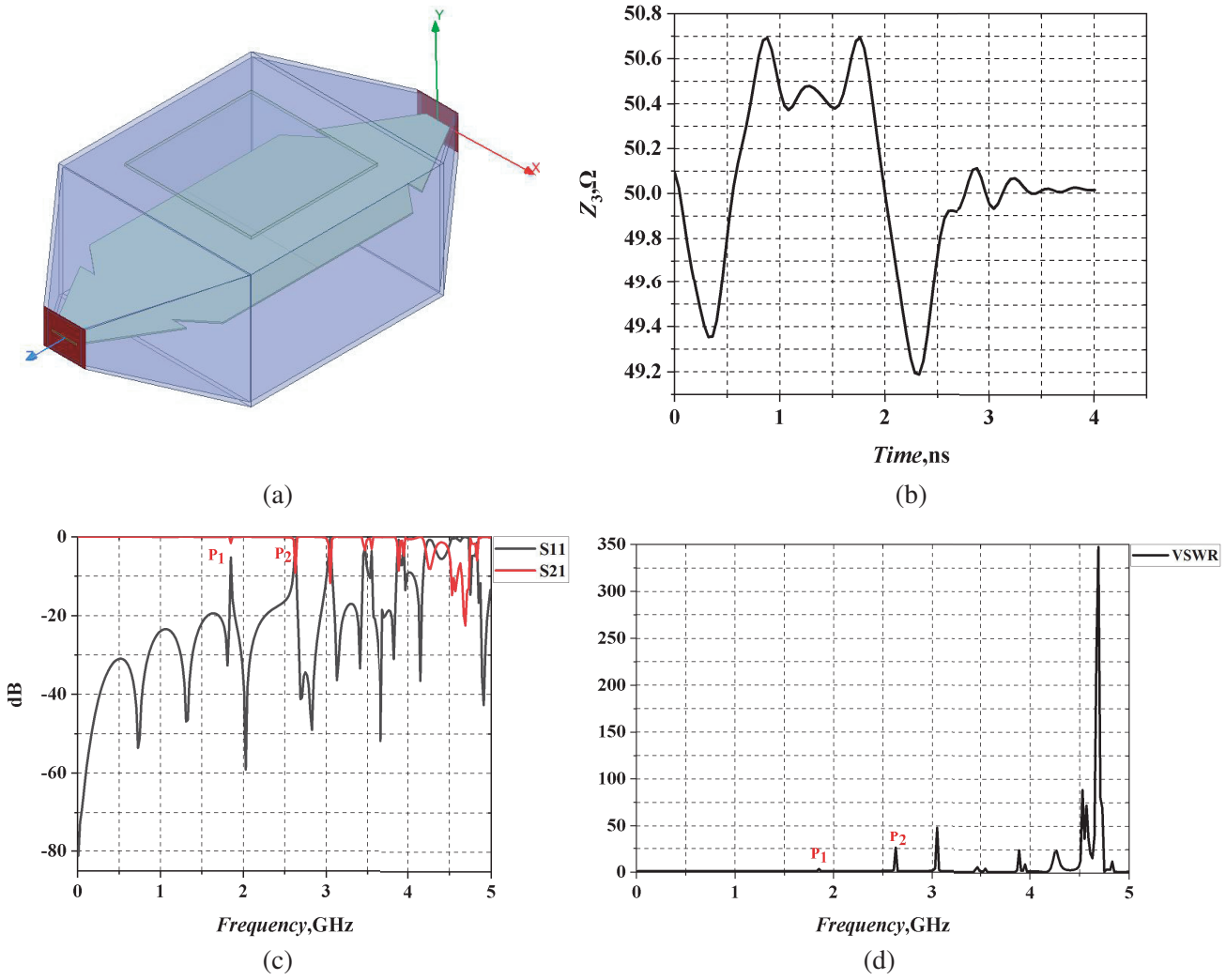

Figure 8. The preliminary designed TEM cell and performance curves of the preliminary designed TEM cell. (a) The preliminary designed TEM cell. (b) Transient impedance Z_3. (c) S-parameters. (d) VSWR.

the cell [12]. When there are five longitudinal slits at the front and rear sides of the middle section, seven longitudinal slits at the bottom, the high-order modes in the cell can be suppressed. The TEM cell model after the slit design, S-parameters, and VSWR results are shown in Fig. 9. In the range of 0–3 GHz, the S_{11} of peak P_3 is −17.51 dB at 1.67 GHz. At the same time, the corresponding VSWR is 1.31 at 1.67 GHz. Compared with the preliminary designed TEM cell, the original resonance peaks P_1 and P_2 are eliminated, and the peak value of the VSWR in the whole simulation frequency range is reduced from 347.40 to 7.35. The results show that opening longitudinal slits on the outer conductor can cut off the high-order mode currents and effectively suppress the high-order modes within the working bandwidth.

TEM cell is a nonuniform structure, wave reflection is easy to occur at the junction of the rectangular middle section and the tapered transition section. Considering that without affecting the test space, a small piece of absorbing material is loaded at the junction to absorb the reflect waves and further suppress high-order modes. The TEM cell model with slits and absorbing materials, S-parameters, and VSWR results are shown in Fig. 10. In the range of 0–3 GHz, the S_{11} of peak P_4 is −18.86 dB at 1.69 GHz. At the same time, the corresponding VSWR is 1.26 at 1.69 GHz. Compared

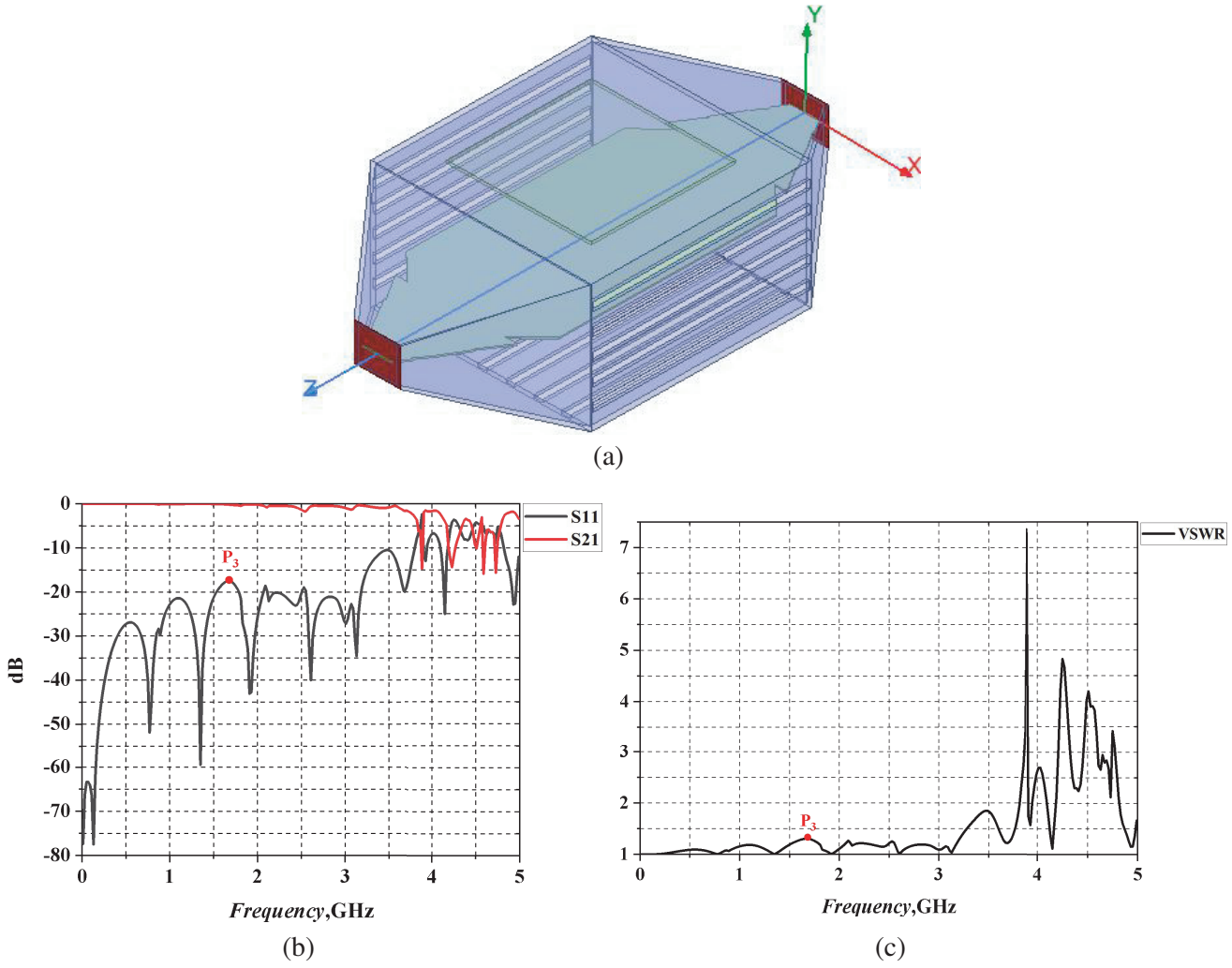

Figure 9. The TEM cell model after the slit design, S-parameters and VSWR results. (a) The TEM cell model after the slit design. (b) S-parameters. (c) VSWR.

with the TEM cell with only slits, the S-parameters and VSWR have no obvious changes in the low frequency band. However, in the whole simulation frequency range, the peak value of VSWR after loading the absorbing materials decreases significantly from 7.35 to 3.08. The results show that loading the absorbing materials can further suppress the resonance in the cell caused by high-order modes and reflection phenomena.

3.2. Slotting Form Adjustment

In order to further reduce VSWR and improve S-parameter characteristics, the inner conductor slotting form can be adjusted. The former slotting form usually has acute angle, which can be converted into obtuse angle for further improvement. The inner conductor with the form of obtuse angle, S-parameters, and VSWR results are shown in Fig. 11. In the range of 0–3 GHz, the S_{11} of peak P_5 is -21 dB at 2.89 GHz. At the same time, the corresponding VSWR is 1.19 at 2.89 GHz. Compared with the TEM cell with acute angle slots, the peak values of S-parameters and VSWR in the low frequency band are further reduced, and the peak value of VSWR is reduced from 1.26 to 1.19.

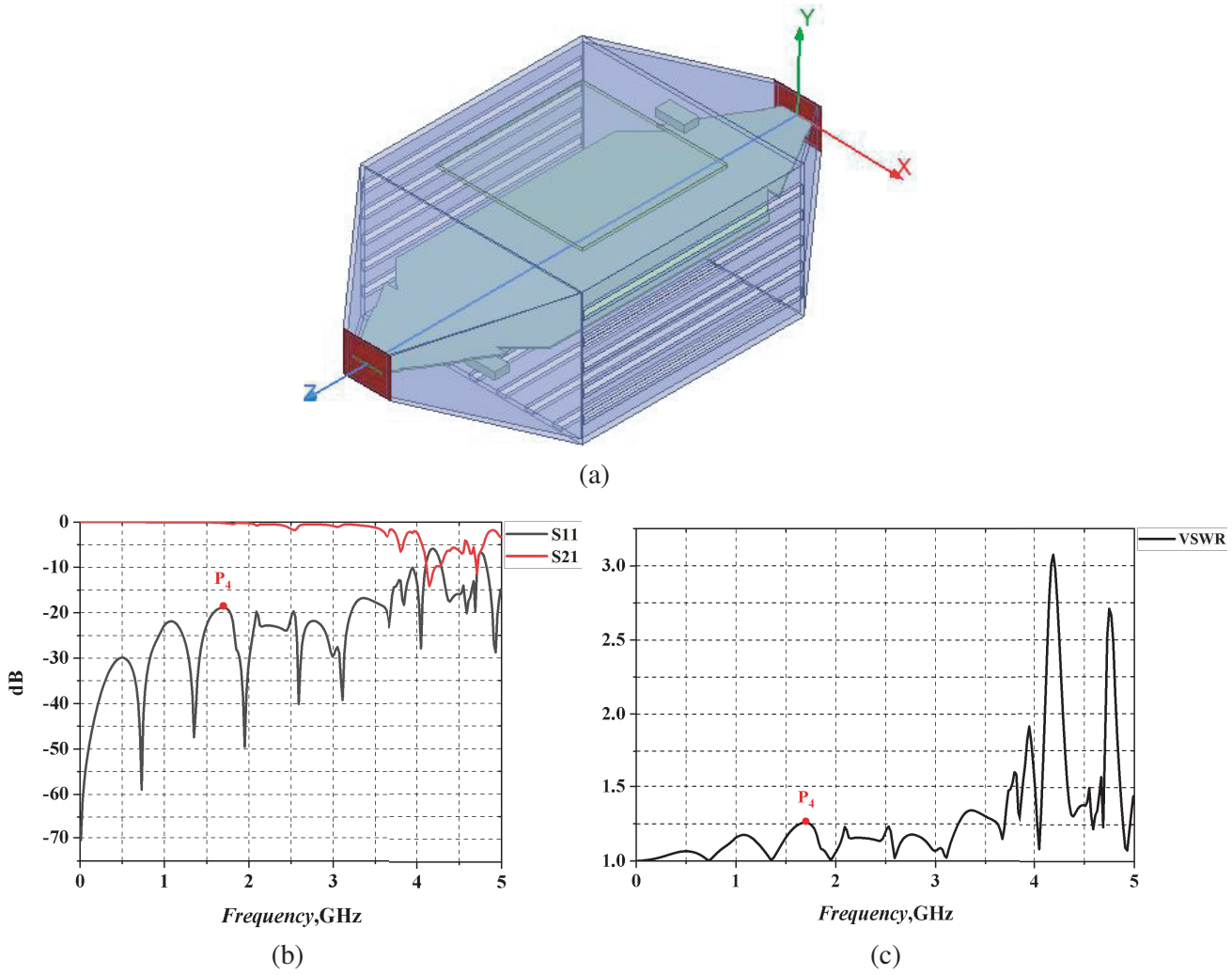

Figure 10. The TEM cell model with slits and absorbing materials, S-parameters and VSWR results. (a) The TEM cell model with slits and absorbing materials. (b) S-parameters. (c) VSWR.

3.3. Adding Outer Shielding Box

Due to surfaces slits, the above designed TEM cell is easy to produce electromagnetic leakage at slits and cannot be well isolated from the external environment. A TEM cell with an external copper shielding box which is covered with absorbing materials, and The final designed TEM cell is shown in Fig. 12, with an external shielding box outside and absorbing materials inside; the corresponding VSWR is shown in Fig. 12(b). With external shielding box, the leakage of TEM cell is minimized, and the external interference is suppressed. According to Fig. 12, in the range of 0–3.4 GHz, the VSWR of peak P_6 is less than 1.2.

4. FIELD DISTRIBUTION CALCULATION OF TEM CELL

According to the main form of transmission waves, TEM cell belongs to vertical device (there is no electric and magnetic field components in the propagation direction of TEM, and the TEM plane is perpendicular to its propagation direction in cell or transmission line). According to IEC61967-2 standard, the field is very uniform in about one third of the volume between the inner conductor and outer conductor of the TEM cell. The structure of the TEM cell is symmetrical, so only the horizontal

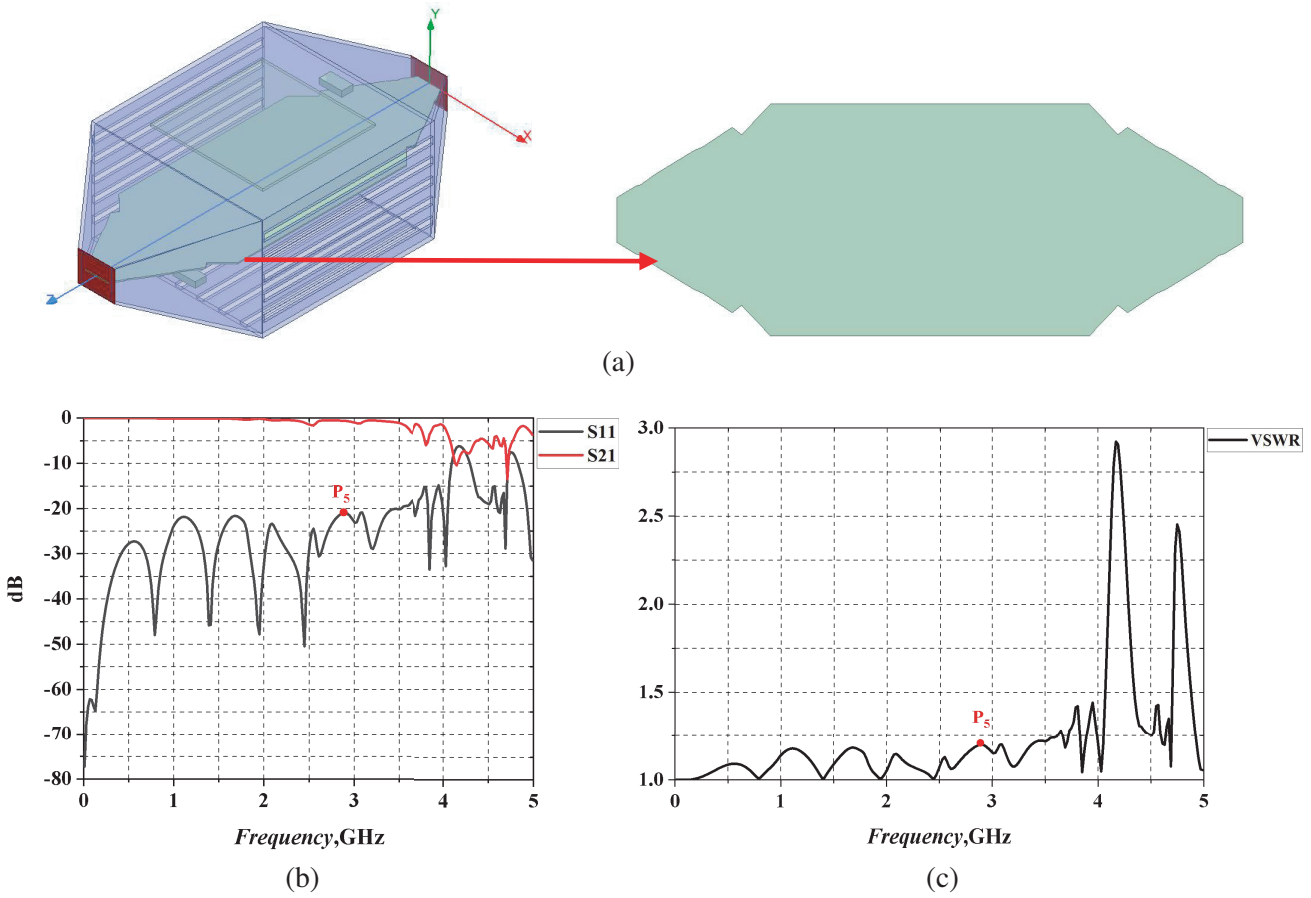

Figure 11. The inner conductor with the form of obtuse angle, *S*-parameters and VSWR results. (a) The inner conductors with the form of obtuse angle. (b) *S*-parameters. (c) VSWR.

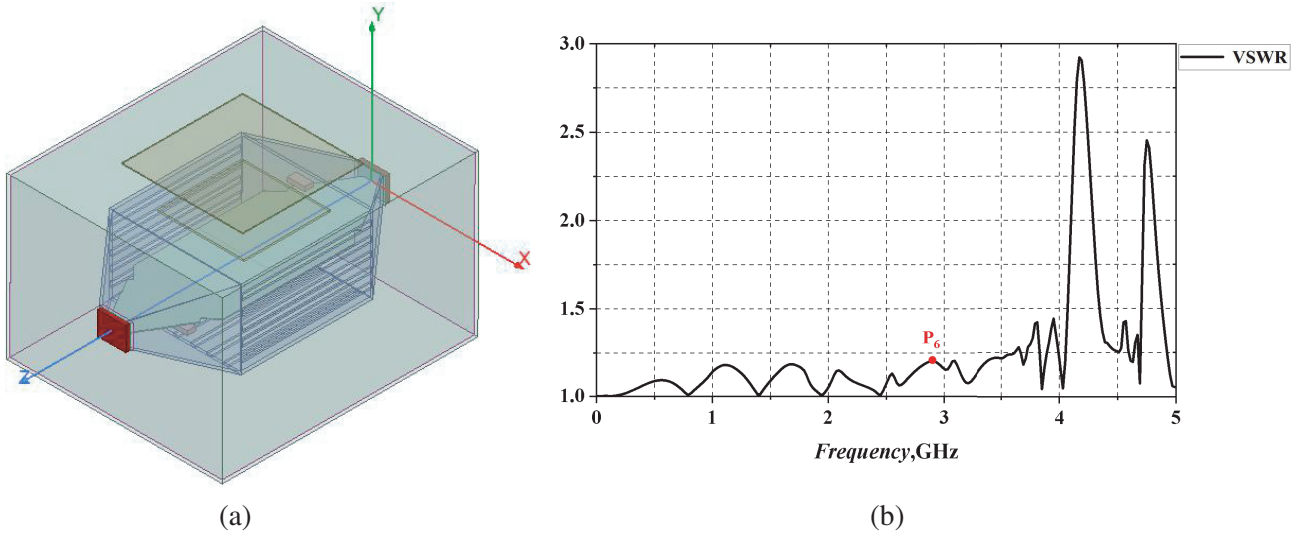

Figure 12. Final designed TEM cell and VSWR result. (a) A TEM cell with an external copper shielding box and the box is covered with absorbing materials. (b) VSWR.

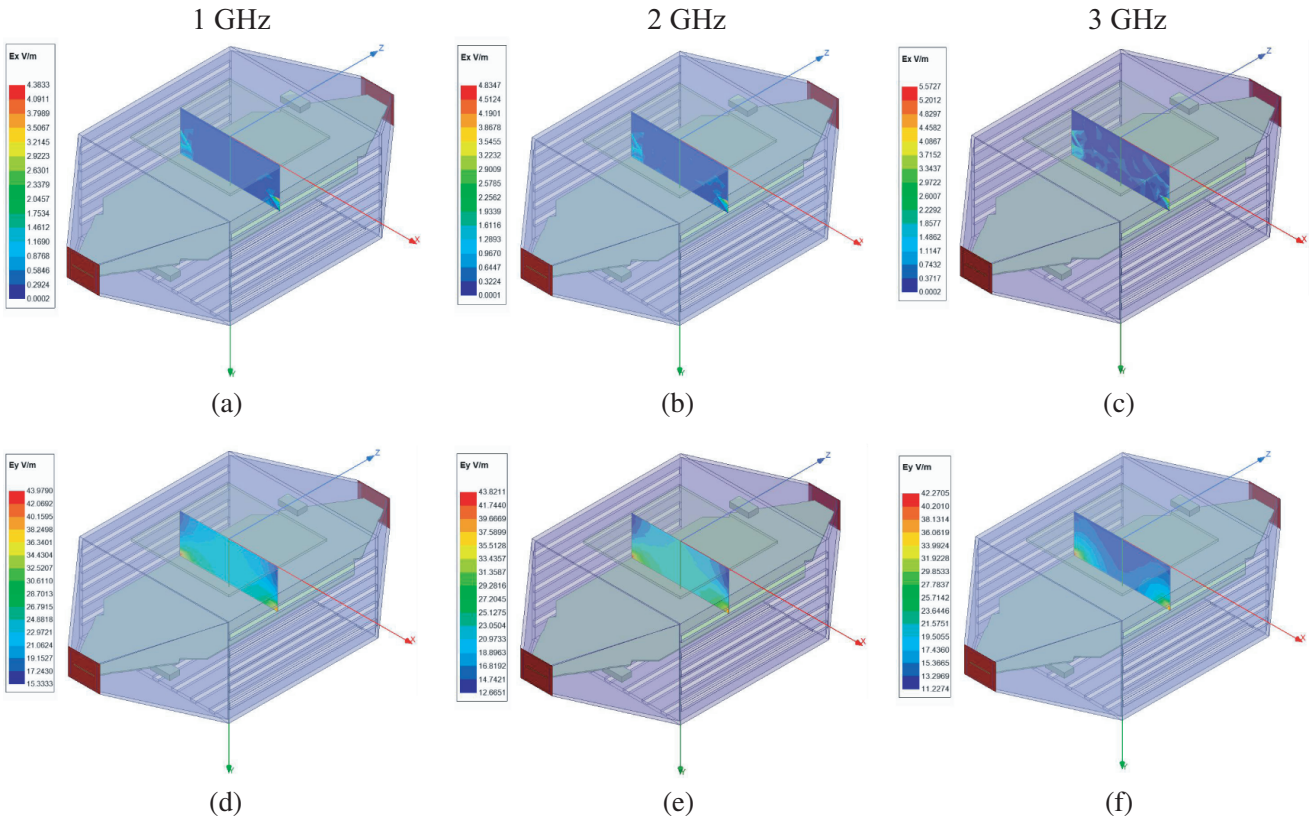

Figure 13. The Ex and Ey at three frequency points. (a) Ex, 1 GHz. (b) Ex, 2 GHz. (c) Ex, 3 GHz. (d) Ey, 1 GHz. (e) Ey, 2 GHz. (f) Ey, 3 GHz.

electric field components (Ex) and vertical electric field components (Ey) of the upper half cell need to be calculated. The Ex and Ey at three frequency points in the measurement range are shown in Fig. 13, and the length (x-axis) and width (y-axis) of the measuring plane are 100 mm and 40 mm, respectively. According to Fig. 13, the Ex is much smaller than the Ey in the measurement range; in the range of $-30\,\text{mm} < x < 30\,\text{mm}$ and $0\,\text{mm} < y < 30\,\text{mm}$, the Ex at three frequency points can be ignored, and the Ey changes little, which indicates that the field in this region has good uniformity and meets the requirements of field uniformity in one third of the volume; when $|x| > 40\,\text{mm}$, the Ey changes greatly, which will affect the reliability of test results.

5. CONCLUSION

In this paper, a TEM cell with VSWR less than 1.2 in 0–3.4 GHz, less than 1.3 in 0–3.75 GHz, and less than 1.5 in 0–4.06 GHz is designed. Compared with the original TEM cell with VSWR of 1.5 in the range of 150 kHz–1 GHz in IEC61967-2 standard, the results show that the upper limit of cell usage frequency with slit outer conductor, slotted inner conductor, absorbing materials, and an external shielding box is significantly improved, and the performance is significantly optimized. To a certain extent, the influence of high-order modes and reflection is weakened, and the requirement of cell verticality is satisfied.

ACKNOWLEDGMENT

This research was funded by the National Natural Science Foundation of China, 61974077 and 61804084.

REFERENCES

1. Song, C. J., X. Y. Feng, and F. Dai, "TEM cell frequency expansion method based on waveguide slot antenna," Vol. 44, No. 302(04), 136–142.
2. International Electrotechnical Commission, "IEC61967-2 Integrated circuits-Measurement of electromagnetic emissions, 150 kHz to 1 GHz — Part 2: Measurement of radiated emissions, TEM-cell and wideband TEM-cell method," Geneva, Switzerland, 2005.
3. Deng, S., D. Pommerenke, T. Hubing, et al., "An experimental investigation of higher order mode suppression in TEM Cells," *IEEE Transactions on Electromagnetic Compatibility*, Vol. 50, No. 2, 416–419, 2008.
4. Koohestani, M., M. Ramdani, and R. Perdriau, "Impact of mode propagation on radiated immunity characterization in commonly used TEM cells," *2019 12th International Workshop on the Electromagnetic Compatibility of Integrated Circuits (EMC Compo)*, 6–8, 2019.
5. Luo, W., Y. L. Guan, and J. Li, "Three new strip-line TEM cells in EMC test," *2016 IEEE International Conference on Electronic Information and Communication Technology (ICEICT)*, 497–500, 2016.
6. Arezoomand, M., M. K. Meybodi, and N. Noori, "Design of a TEM cell using both multi-step and piecewise linear tapering," *2016 8th International Symposium on Telecommunications (IST)*, 2016.
7. Crawford, M. L., J. L. Workman, and C. J. Thomas, "Expanding the bandwidth of TEM cells for EMC measurements," *IEEE Transactions on Electromagnetic Compatibility*, Vol. 20, No. 3, 368–375, 2007.
8. Walter, A. J. and C. Leat, "Control of the TE_{111} resonance in an asymmetric TEM cell," *IEEE Transactions on Electromagnetic Compatibility*, Vol. 50, No. 2, 431–434, 2008.
9. Tippet, J. C. and D. C. Chang, "A new approximation for the capacitance of a rectangular-coaxial-strip transmission line," *IEEE Transactions on Microwave Theory & Techniques*, Vol. 14, No. 9, 602–604, 1976.
10. Chen, J., F. Y. Wan, and P. Fan, "Design of novel broadband TEM cell," *Journal of Hefei University of Technology (Natural Science)*, Vol. 39, No. 7, 938–942, 2016.
11. Su, D. L., A. X. Chen, S. G. Xie, et al., *Electromagnetic Field and Electromagnetic Wave*, 349–356, Higher Education Press, Beijing, 2008.
12. Quan, S. H., *The Basis of Microwave Technology*, 155–157, Higher Education Press, Beijing, 2011.